TECHNICAL PAPER

ISSN:1047-3289 *J. Air & Waste Manage. Assoc.* **57**:1360–1369
DOI:10.3155/1047-3289.57.11.1360

Estimating Fine Particulate Matter Component Concentrations and Size Distributions Using Satellite-Retrieved Fractional Aerosol Optical Depth: Part 2—A Case Study

Yang Liu and Petros Koutrakis
Harvard School of Public Health, Boston, MA

Ralph Kahn
Jet Propulsion Laboratory, California Institute of Technology, Pasadena, CA

Solene Turquety
Université Pierre et Marie Curie, Paris, France

Robert M. Yantosca
Harvard Division of Engineering and Applied Sciences, Cambridge, MA

ABSTRACT

We use the fractional aerosol optical depth (AOD) values derived from Multiangle Imaging Spectroradiometer (MISR) aerosol component measurements, along with aerosol transport model constraints, to estimate ground-level concentrations of fine particulate matter ($PM_{2.5}$) mass and its major constituents in the continental United States. Regression models using fractional AODs predict $PM_{2.5}$ mass and sulfate (SO_4) concentrations in both the eastern and western United States, and nitrate (NO_3) concentrations in the western United States reasonably well, compared with the available ground-level U.S. Environment Protection Agency (EPA) measurements. These models show substantially improved predictive power when compared with similar models using total-column AOD as a single predictor, especially in the western United States. The relative contributions of the MISR aerosol components in these regression models are used to estimate size distributions of EPA $PM_{2.5}$ species. This method captures the overall shapes of the size distributions of $PM_{2.5}$ mass and SO_4 particles in the east and west, and NO_3 particles in the west. However, the estimated $PM_{2.5}$ and SO_4 mode diameters are smaller than those previously reported by monitoring studies conducted at ground level. This is likely due to the satellite sampling bias caused by the inability to retrieve aerosols through cloud cover, and the impact of particle hygroscopicity on measured particle size distributions at ground level.

IMPLICATIONS

This paper examines the ability of MISR fractional AODs to predict ground-level concentrations and size distributions of $PM_{2.5}$ and its major constituents. Our results suggest that MISR fractional AOD data can become a valuable resource in our effort to determine the time and space-resolved $PM_{2.5}$ exposure. Aerosol vertical profiles simulated by atmospheric chemical transport models can improve the association between MISR fractional AODs and ground $PM_{2.5}$ information.

INTRODUCTION

There have been many epidemiologic studies examining the health effects of fine particulate matter ($PM_{2.5}$, particles less than 2.5 μm in diameter) since 1997.[1] Measuring the characteristics of $PM_{2.5}$, including chemical composition and size distribution, is crucial in determining the relative toxicity of different $PM_{2.5}$ constituents, hence developing cost-effective emission control policies. However, particle chemical characterization over large regions is limited because it is costly and time consuming. Furthermore, $PM_{2.5}$ size distribution is not routinely measured by most ground monitoring networks. Available information in the peer-reviewed literature is mostly from intensive measurement campaigns (e.g., U.S. Environmental Protection Agency [EPA] PM supersites) over short periods.

Earth observing satellites can cover nearly the entire globe in the matter of a few days. The rapidly advancing satellite aerosol remote sensing technology makes them a potential source of information on the transport and spatial patterns of particles. The aerosol optical depth (AOD) retrieved by the Moderate Resolution Imaging Spectroradiometer (MODIS) has been reported to be correlated with $PM_{2.5}$ mass concentrations in the United States and this correlation is stronger on the East Coast.[2] An assessment over 26 locations in five countries shows that ground $PM_{2.5}$ concentrations and the bin-averaged daily mean MODIS AOD have a linear correlation coefficient of 0.96.[3] Liu et al. developed multivariate regression models to compare the capability of MODIS AOD in predicting

ground $PM_{2.5}$ concentrations with AOD retrieved by the Multiangle Imaging Spectroradiometer (MISR) aboard NASA's EOS Terra satellite in the St. Louis metropolitan area.[4] The two models have comparable regression coefficients with MISR having a slightly higher predicting power as indicated by the model R^2. This paper presents the results of a case study in which we estimate ground-level concentrations of $PM_{2.5}$ and its major constituents using the fractional AOD derived from the MISR aboard NASA's EOS Terra satellite. We chose the continental United States as our modeling domain and collected $PM_{2.5}$ speciation data measured by EPA's Speciation and Transport Network (STN) in 2005.

DATA AND METHODS

MISR Level 2 Aerosol Data

MISR Level 2 aerosol data (MIL2ASAE, Version 17) covering the continental United States in 2005, MISR Aerosol Physical and Optical Properties (APOP) file and the Aerosol Mixture file were downloaded from the NASA Langley Research Center (LARC) Atmospheric Sciences Data Center (*edg.larc.nasa.gov/~imswww/imswelcome/index.html*). MISR retrieves aerosol properties by first assuming a set of aerosol models (called "mixtures of aerosol components" in MISR literature) in the atmosphere. For each MISR observation at a given location and time, top-of-atmosphere radiances simulated for each mixture are computed and compared with the MISR observations to determine those mixtures that provide good fits to the data, that is, the "successful mixtures".[5] These mixtures are created by externally mixing up to three individual aerosol components defined by a size distribution, shape, complex index of refraction, and scale height. The percentage contributions of all the components to the AOD corresponding to a mixture sums to one. As for Version 17 data, eight aerosol components (i.e., component 1, 2, 3, 6, 8, 14, 19, and 21) are used to construct a total of 74 aerosol mixtures. The MIL2ASAE data product provides AOD values and success flags (i.e., whether a mixture is considered a good fit to the observation) for all aerosol mixtures. The APOP file and Aerosol Mixture file contain detailed information on the aerosol components that are used to construct the aerosol models, and the percentage contribution of each component to total AOD. A detailed discussion of MISR data structure is given in a companion article.[6]

EPA $PM_{2.5}$ Speciation Data

$PM_{2.5}$ chemical speciation data collected by EPA STN monitors for 2005 were downloaded from EPA's Air Quality System (AQS) databases (*www.epa.gov/ttn/airs/airsaqs/detaildata/downloadaqsdata.htm*, accessed on April 24, 2006). Figure 1 shows the spatial distribution of approximately 130 STN sites with $PM_{2.5}$ measurements after matching with MISR aerosol data. Fewer STN sites in the west result in a smaller dataset in the western United States, which limits the predictors we can include in the regression analysis. Unfortunately, no other data sources are available to supplement the STN data for our modeling period. The Interagency Monitoring of Protected Visual Environments (IMPROVE) program operates a monitoring network that provides similar measurements to EPA's STN network. However, IMPROVE data for 2005 were not available at the time of this analysis. In addition, all IMPROVE sites are located in the National Parks and wilderness areas. Their great distances to populated urban areas make them less useful to this analysis. Parameters used in the current analysis include daily average $PM_{2.5}$ mass concentration measured by gravimetric methods, sulfate (SO_4), nitrate (NO_3), organic carbon (OC), and elemental carbon (EC) concentrations. Preliminary analysis shows that these four species are all highly significant predictors of $PM_{2.5}$ mass ($R^2 = 0.95$). On average, they account for approximately 71% of the total $PM_{2.5}$ mass. The rest of the particle mass may include crustal materials, water, and other unknown materials. We use silicon concentrations as a surrogate of mineral dust in our analysis,

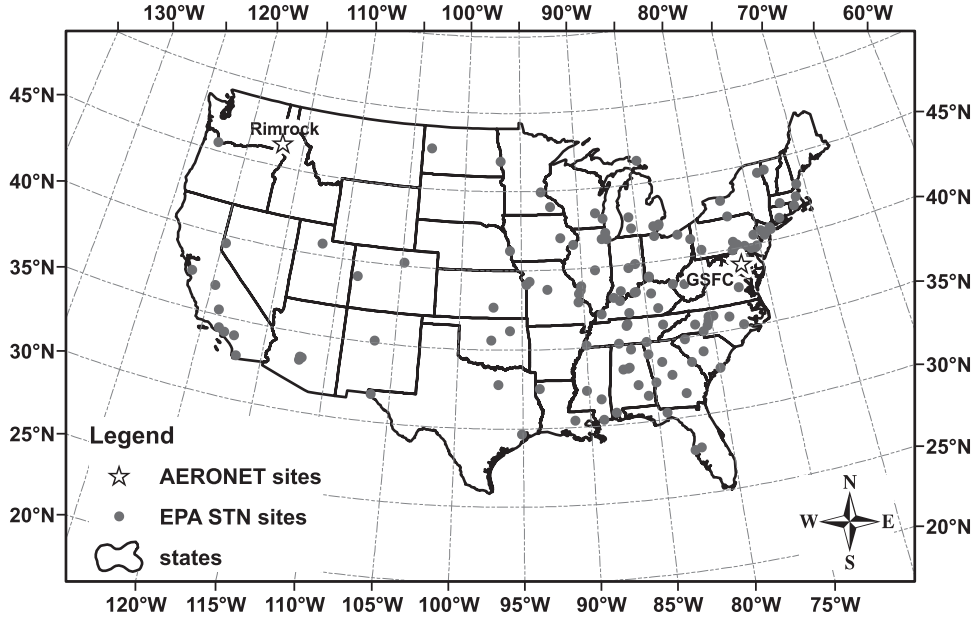

Figure 1. Geographical locations of EPA STN sites and the AERONET sites used to validate MISR-derived particle size distributions.

as it was shown to be the dominant indicator of soil and crustal materials in urban areas by factor analysis.[7]

STN data records flagged with Quality Assurance qualifiers were excluded because these qualifiers indicate that these data are of low quality. Other qualifiers include Exceptional Event (EX) qualifiers (structural fire, construction or active agricultural activities, cleaning after disasters or accidents, etc. during sample collection) and Natural Events (NAT) qualifiers (forest fires, high winds, etc. during sample collection). In our dataset, there are one structural fire, three construction events, and one agricultural tilling event in the east, and one forest fire in the west. Including the data records flagged with EX qualifiers does not change the parameter estimates but they slightly deteriorate the adjusted R^2 values. This is probably because the spatial resolution of our satellite data and model simulations cannot capture these small-scale events. As a result, we did not include these data records in the final models. Although the data record was flagged with a NAT qualifier, the Cave Creek forest fire started on June 21 near Carefree, AZ did not significantly increase the $PM_{2.5}$ concentration or EC concentration measured on June 27 at the EPA site at Scottscale, AZ, approximately 30 km south of the fire site. Therefore, this data record was included in the final models.

GEOS-Chem Aerosol Simulation Data

Developed at Harvard University, the GEOS-Chem model is a global three-dimensional chemistry and transport model driven by assimilated meteorology. A detailed description of GEOS-Chem and its aerosol simulation can be found elsewhere.[8,9] GEOS-Chem near-real-time run (NRT) results (Version 7-02-04) were obtained from the University of Washington (*coco.atmos.washington.edu/cgi-bin/ion-p?page = geos_nrt.ion*). Output fields used in the current analysis include optical depth of SO_4, nitrate (NO_3), OC, EC, and mineral dust at 3-hr intervals, $2^\circ \times 2.5^\circ$ spatial resolution, and 17 vertical layers in the troposphere. The 3-hr outputs are interpolated to 10:00 a.m. to 11:00 a.m. local time values, which correspond to the MISR observation time window. GEOS-Chem simulated aerosol vertical profiles are used as scaling factors to calculate the fractions of MISR AOD in the lower atmosphere, as discussed later. Ideally, aerosol vertical profiles at a higher spatial resolution should be used for this urban-scale study. However, such data were not available to us at the time of this analysis. Despite the coarse resolution, previous analysis shows that including GEOS-Chem aerosol simulations in the analysis can significantly strengthen the association between MISR AOD and ground-level EPA $PM_{2.5}$ concentrations.[10]

Data Processing and Model Development

Our modeling analysis takes four steps. First, we calculate column fractional AOD for each MISR aerosol component. Second, we estimate lower-air fractional AOD by scaling the column fractional AOD with the simulated aerosol vertical profiles from GEOS-Chem. Third, we build the linear regression models with fractional AOD values as the major predictors of concentrations of $PM_{2.5}$ mass and its major constituents. Finally, we derive particle size distribution information using the regression coefficients. This approach as well as MISR data structure is discussed in detail in the companion article. Data from MISR, EPA, and GEOS-Chem are spatially and temporally matched before analyzing the relationship between MISR fractional AODs and EPA $PM_{2.5}$ speciation information. The fractional AOD of a MISR aerosol component is defined as the average contribution of this component to total AOD over all the aerosol mixtures that provide good fits to MISR observations. It is calculated for those components present in an observation. In this study, we keep all AOD values (558 nm) between 0.15 and 1.5 to be consistent with the sensitivity study presented in the companion article. Among all the valid MISR observations spatially matched to the STN sites, approximately 60% of them have overall AOD values below 0.15. Removing these low AOD values substantially limits our sample size, which results in the reduction of statistical power, and makes our results representative of more polluted conditions. In the companion paper, we used the number of successful aerosol mixtures (i.e., mixtures that pass the selection criteria and are considered good fits to an observation) as an indicator of MISR particle type retrieval error.[6] A MISR observation is considered to have less uncertainty when only a small number of aerosol mixtures are considered good fits to it. For the current dataset, the median number of successful mixtures is eight for the data with total AOD values greater than 0.15 in the east, and 13 in the west. For the data with total AOD values between 0.05 and 0.15, this number is 14 in the east and 24 in the west. Therefore, setting a lower bound of 0.15 for total AOD allowed higher quality MISR particle type information to be included in the modeling process.

We use GEOS-Chem simulated aerosol vertical profiles to compute lower-air fractional AOD for each MISR component. Three of the 17 GEOS-Chem tropospheric layers are within 1 km above the surface. The lower-air AOD proportion is calculated as the sum of simulated AOD values in lowest three layers divided by the total AOD. However, given the differences between the MISR-assumed aerosol components and GEOS-Chem aerosol species, it is impossible to directly scale each of the MISR aerosol components. Instead, we sum GEOS-Chem AOD values for SO_4, NO_3, OC, and EC at each vertical layer to roughly represent the contribution of anthropogenic particles over land. We calculate the ratio of the GEOS-Chem anthropogenic AOD in the lowest three layers over the GEOS-Chem anthropogenic AOD for the whole air column. Then, we multiply the MISR fractional AOD for each of the non-dust components (i.e., 1, 2, 3, 6, 8, and 14) by this ratio to represent the fractional anthropogenic AODs in the lower air. This procedure is summarized in eq 1a and 1b. Similarly, we calculate the ratio of GEOS-Chem dust AOD in the lowest three layers over the total dust AOD, and use it to calculate the fractional AODs for each of the MISR dust aerosol components (19 and 21) in the lower atmosphere.

$$\text{MISR lower-air anthropogenic AOD} = \frac{\text{GEOS-CHEM lower-air anthropogenic AOD}}{\text{GEOS-CHEM column anthropogenic AOD}} \times \text{MISR non-dust AOD} \quad (1a)$$

where MISR anthropogenic AODs refer to the fractional AODs for components 1, 2, 3, 6, 8, and 14.

$$\text{MISR lower-air dust AOD} = \frac{\text{GEOS-CHEM lower-air dust AOD}}{\text{GEOS-CHEM column dust AOD}} \times \text{MISR dust AOD} \quad (1b)$$

where MISR dust AODs refer to the fractional AODs for components 19 and 21.

The scaled lower-air MISR AODs are used in the subsequent modeling process. We refer to them as MISR fractional AODs for simplicity. Detailed model development is presented in the companion article, so it is not repeated here. Before removing the outliers, there are 208 and 56 observations in the eastern and western United States (95 ° longitude as the division line), respectively. Given the small size of the datasets, only a binary seasonal indicator is included in all the models to account for the impact of relative humidity (RH; see eq 2). The seasonal indicator equals 1 representing high RH seasons (summer and fall, i.e., from June to November), or 0 representing low RH seasons (winter and spring, i.e., from December to May). The Cook's D threshold is set at the 20th percentile value, which is generally between 0.3 and 0.6, and the outliers are discussed separately. Model performance is evaluated by adjusted R^2, which penalizes the inclusion of more predictor variables in a model.

$$\text{STN } PM_{2.5} \text{ Constituent Concentration} = \beta_0 + \sum_{i=1}^{8} \beta_i \times \text{MISR fractional AOD}_i + \beta_9 \times \text{Seasonal Indicator} \quad (2)$$

RESULTS AND DISCUSSION

Relationships between $PM_{2.5}$ Components and Fractional AODs

Tables 1 and 2 show the modeling results between EPA observations of $PM_{2.5}$ constituent concentrations and fractional MISR AODs in the east and west, respectively. The EC and silicon models do not produce any meaningful results because of their low concentration levels and severely reduced datasets caused by many zero values in the EPA data. Therefore, they are not listed here. All fractional AOD variables with positive regression coefficients that are significant at the $\alpha = 0.25$ level are included in the final models. The statistical significance of model intercept is also evaluated at the $\alpha = 0.25$ level. Results of similar models with total MISR AODs scaled by GEOS-Chem aerosol profiles are given as a comparison. All the models are highly significant (p value < 0.0001).

Table 1. Regression results of the fractional AOD models and the total AOD models in the eastern United States after removing outliers.

	Fractional AOD Model				Total AOD Model			
Dependent Variable	***N*[a]**	**Adjusted R^2**	**Predictor Variable**	**Regression Coefficient (SE)**	***N***	**Adjusted R^2**	**Predictor Variable**	**Regression Coefficient (SE)**
$PM_{2.5}$	203	0.56	Intercept	5.2 (1.1)[c]	207	0.42	Intercept	8.0 (1.1)[c]
			AOD_1[b]	206.8 (29.7)[c]			AOD_{total}	57.8 (6.5)[c]
			AOD_2	123.5 (10.7)[c]			High RH Season	5.7 (1.0)[c]
			AOD_3	68.9 (10.5)[c]				
			AOD_8	108.6 (16.3)[c]				
			AOD_{14}	92.1 (37.1)[d]				
			High RH Season	4.3 (0.9)[c]				
SO_4	206	0.62	AOD_1	120.2 (12.6)[c]	206	0.43	AOD_{total}	26.9 (2.8)[c]
			AOD_2	58.7 (4.3)[c]			High RH Season	2.2 (0.5)[c]
			AOD_3	43.7 (4.4)[c]				
			AOD_8	55.5 (7.0)[c]				
			AOD_{21}	135.2 (74.1) ($P = 0.07$)				
			High RH Season	0.9 (0.4)[d]				
NO_3	206	0.13	Intercept	1.2 (0.3)[c]	204	0.11	AOD_{total}	2.5 (1.4) ($P = 0.07$)
			AOD_2	3.5 (2.5) ($P = 0.17$)			High RH Season	−1.1 (0.2)[c]
			AOD_8	6.5 (4.2) ($P = 0.12$)				
			AOD_{14}	32.7 (9.7)[c]				
			High RH Season	−1.0 (0.2)[c]				
OC	206	0.19	Intercept	3.8 (0.3)[c]	206	0.15	Intercept	4.2 (0.3)[c]
			AOD_1	16.1 (8.0)[d]			AOD_{total}	2.0 (1.6) ($P = 0.23$)
			AOD_2	10.0 (2.6)[c]			High RH Season	1.4 (0.3)[c]
			AOD_8	8.5 (4.5)[d]				
			High RH Season	1.0 (0.3)[c]				

Notes: [a]*N* represents the sample size after removing the potential outliers. [b]AOD_1 is the fractional AOD of MISR component 1. Similarly, AOD_2 is fractional AOD of MISR component 2, and so on. [c]Significant at the $\alpha = 0.001$ level; [d]significant at the $\alpha = 0.05$ level.

Table 2. Regression results of the fractional AOD models and the total AOD models in the western United States after removing outliers.

	Fractional AOD Model				Total AOD Model			
Dependent Variable	***N***	**Adjusted R^2**	**Predictor Variable**	**Regression Coefficient (SE)**	***N***	**Adjusted R^2**	**Predictor Variable**	**Regression Coefficient (SE)**
$PM_{2.5}$	53	0.57	AOD_2	142.1 (20.7)[a]	54	0.21	AOD_{total}	91.9 (23.1)[a]
			AOD_3	198.1 (36.0)[a]			High RH Season	2.0 (1.8) ($P = 0.25$)
			AOD_6	97.5 (28.6)[b]				–
			AOD_8	145.6 (47.3)[b]				–
			AOD_{21}	541.5 (165.8)[b]				–
SO_4	54	0.40	AOD_1	74.3 (33.8)[c]	54	0.11	AOD_{total}	16.8 (6.3)[b]
			AOD_2	41.7 (7.0)[a]			High RH Season	0.7 (0.5) ($P = 0.22$)
			AOD_3	20.6 (10.5)[c]				
			AOD_8	32.4 (17.1)[c]				
			AOD_{21}	165.1 (56.8)[b]				
NO_3	54	0.54	AOD_3	94.8 (15.6)[a]	54	0.23	Intercept	−3.1 (1.3)[c]
			AOD_6	26.3 (12.8)[c]			AOD_{total}	39.8 (9.6)[b]
			AOD_{19}	54.2 (16.7)[b]				
			High RH Season	−0.8 (0.6) ($P = 0.16$)				
OC	56	0.28	Intercept	2.4 (0.5)[a]	54	0.11	Intercept	1.9 (0.8)[c]
			AOD_2	20.4 (7.2)[b]			AOD_{total}	14.6 (6.0)[c]
			AOD_3	37.0 (9.5)[a]			High RH Season	0.8 (0.4) ($P = 0.07$)
			AOD_8	18.5 (15.4) ($P = 0.23$)				
			High RH Season	0.8 (0.5) ($P = 0.09$)				

Notes: [a]Significant at the $\alpha = 0.001$ level, [b]significant at the $\alpha = 0.01$ level, [c]significant at the $\alpha = 0.05$ level.

The adjusted R^2 values indicate that after adjusting for the number of predictors included in the models, the fractional AOD models are able to explain 13–62% of the variability in the concentrations of $PM_{2.5}$ mass and its major constituents in the eastern United States, and 28–56% in the western United States. The predicting powers of the fractional AOD models are moderately greater than their corresponding total AOD models in the east, and substantially greater in the west. The improvements of adjusted R^2 values range between 19% (NO_3 model) and 44% (SO_4 model) in the east, and between 129% (NO_3 model) and 233% (SO_4 model) in the west. The seasonal effects in the east are highly significant and the regression coefficients of the seasonal indicator are similar in both sets of models. In the west, the seasonal effect is generally either weak or insignificant in both sets of models. In most previous studies that intend to link AOD and near-surface $PM_{2.5}$ measurements, total-column AOD was used as one predictor of ground level $PM_{2.5}$ concentrations.[2,4,11,12] Our finding suggests that using total AOD as a single predictor could introduce a substantial amount of uncertainty because it weighs all aerosol components equally and does not consider the impact of changing particle composition on the association between AOD and $PM_{2.5}$. In the context of our regression models, using AOD as the sole predictor of particle abundance means assuming all the aerosol components to be significant predictors and having identical regression coefficients. As a result, it is not surprising to see that the fractional AOD models, which are much more flexible in adjusting for the changing particle composition, show dramatically improved capability in explaining the variability of the concentrations of $PM_{2.5}$ constituents as compared with the total AOD models.

In the east, MISR aerosol components are more strongly associated with $PM_{2.5}$ mass and SO_4 concentrations than with NO_3 and OC, as indicated by the adjusted R^2. The seasonal indicator is significant in all the models. The darkest MISR component, No.14, is significant in the $PM_{2.5}$ model, which probably accounts for the light-absorbing carbonaceous particles such as the small amount of EC and some light-absorbing OC components. In the west, MISR components are more strongly associated with $PM_{2.5}$ total mass, SO_4, and NO_3 concentrations than with OC concentrations. The seasonal indicator is not significant in the $PM_{2.5}$ and SO_4 model. The definitions of MISR aerosol components are distinguished by size, shape, and single-scattering albedo, but not by chemical composition, which makes it difficult to interpret the significant predictors in these models in terms of particle chemistry. The significance of dust components (19 and 21) in the SO_4 models and the NO_3 model in the west (see Tables 1 and 2) could be caused by the particles having the dust component size distributions and shapes. In addition, the composition and microphysical properties of SO_4 and NO_3 are relatively simple and well documented. In contrast, the microphysical properties of OC particles are more varied and less well known than inorganic particles.[13] Consequently, MISR is less capable of distinguishing light absorbing mixtures from non-light-absorbing mixtures, as shown by the results in the companion article.

Model biases are estimated by linear regression between the fitted values and the observations. As an example, Figure 2 shows the scatter plots of fitted $PM_{2.5}$ mass and SO_4 concentrations in the east and west versus respective EPA observations (i.e., the four models with the largest adjusted R^2). After removing the outliers, the $PM_{2.5}$ models underpredict $PM_{2.5}$ concentrations by approximately 7–8% in both the east and the west. The SO_4

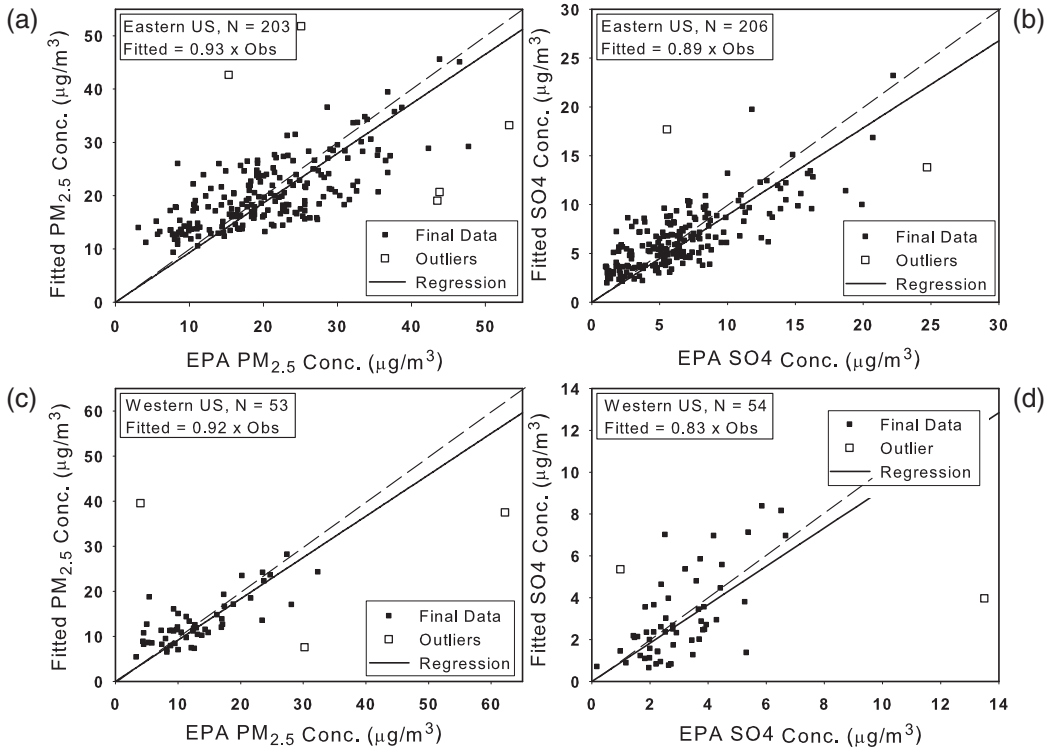

Figure 2. Scatterplots of fitted $PM_{2.5}$ mass in (a) the eastern and (c) western United States, and SO_4 concentrations versus EPA observations in (b) the eastern and (d) western United States. Solid lines represent simple linear regression results with intercepts excluded. The 1:1 lines are displayed as dashed lines for reference. Final data used to derive the regression coefficients are displayed as small black squares and outliers are displayed as large hollow squares.

model underestimates by approximately 10% in the east and approximately 17% in the west. The model relative error (model root-mean-square error divided by observed mean concentration of dependent variable) is approximately 30% for $PM_{2.5}$ in the east, 34% in the west, 39% for SO_4 in the east, and 51% for SO_4 in the west.

The results of our analysis apparently indicate that MISR aerosol components have different relative influences on particle mass (i.e., MISR aerosol components have different regression coefficients in the linear models). The regional variation of particle compositions is also clearly seen by the different regression coefficients in the east from the west. Although there are statistically insignificant components that do not seem to contribute to fine particle mass in one region (e.g., components 6 and 19 in the east), these components may become significant in other regions. It should be noted that only MISR provides aerosol-type-specific fractional AOD values, which enables us to examine the predictability of different aerosol components on fine particle mass concentrations. The results of the current analysis cannot be directly applied to aerosol data retrieved by other current satellite sensors such as POLDER (Polarization and Directionality of the Earth's Reflectances), which reports microphysical properties only for particles smaller than 0.35 μm; MODIS, which reports only fine/coarse aerosol ratio;[10] or the Geostationary Operational Environmental Satellites (GOES). Nonetheless, including any available indicators of particle composition is likely to improve the results of air quality monitoring analyses from these sensors. Because the Ozone Measurement Instrument (OMI) aboard NASA's Aura satellite reports both extinction and absorption optical depth, the method discussed in the current paper might also help better utilize the OMI aerosol data.

When the MISR data with total AOD values greater than 0.05 were included in the models, these models yielded similar regression coefficients and adjusted R^2 values (results not shown). This is probably because these data points are near the lower end of the AOD value range so they do not have enough leverage to change the estimated regression coefficients. Caution must be given when applying the results of this paper to lower AOD values because the MISR particle-type retrieval errors are greater in these observations, as previously mentioned.

In addition to the uncertainties in MISR aerosol retrieval, the performance of these models might also be influenced by the aerosol vertical profile, particle growth at increased RH, and the uncertainties of STN measurements. It has been shown that aerosol vertical distribution does not significantly impact satellite retrieved column-average aerosol microphysical properties, at least when weakly absorbing species are dominant and away from optically thick aerosol plumes.[14] Previous results show that using GEOS-Chem vertical profiles to scale MISR AOD values improves model performance, which is probably because the scaling procedure can partially account for the vertical profiles of different aerosol species.[10] Aerosol hygroscopicity can be a factor because the satellite retrieves AOD under ambient conditions, whereas the EPA $PM_{2.5}$ measurements are made

in a controlled, low RH environment (although measured $PM_{2.5}$ mass still contains an unknown amount of water).[15] This discrepancy in measurement methods could be substantial especially when the RH is high in the boundary layer, unless RH correction factors are included in the models. The significance of the seasonal indicator in all the models may reflect the impact of RH on the associations. Unfortunately, the small size of our dataset limits the number of predictors such as RH. This issue will be pursued in future research, using larger samples and more mature MISR particle property products. Among the STN $PM_{2.5}$ speciation measurements, SO_4 measurements are probably the most stable because SO_4 is nonvolatile. A large amount of NO_3 may be lost during sampling because of vaporization during warm seasons. OC is a mixture of hundreds of different organic compounds, whose concentration is not directly measured, but estimated with a thermal/optical transmittance (TOT) technique. OC concentration is likely the most uncertain of the major $PM_{2.5}$ constituents.[16] This could partially be attributed to the lower adjusted R^2 of the OC models.

Analysis of Model Outliers

Using the Cook's D thresholds and studentized residuals, five outliers are identified for the $PM_{2.5}$ model in the east (~2% of the dataset), as shown in Figure 2a, two of which are also outliers for the SO_4 model (~1% of the dataset). The number of successful aerosol mixtures in the MISR retrievals ranges from 2 to 13, suggesting that it is not an important factor in identifying outliers. These outliers were all measured around the Great Lakes. Al-Saadi et al.[2] have reported similar cases with MODIS data between Lakes Superior and Michigan. When assessed with additional meteorological information, the authors attribute these outliers to the impact of the land-water boundary, which results in aerosol intrusion layers aloft, and weakens the correlation between AOD and ground level $PM_{2.5}$ concentrations. Three outliers are identified in the west (~5% of the dataset), as shown in Figure 2b; two of these are also outliers in the NO_3 model (~4% of the dataset). Possible causes of these outliers might include isolated pollution episodes occurring beyond the MISR sampling time window, and MISR's insensitivity to the aerosol mixtures under certain circumstances. Although many data samples are collected near the eastern and western seashores, they do not appear to be outliers. The inclusion of GEOS-Chem simulated aerosol vertical profiles might help alleviate the effect of large-scale land-water interactions, but it is probably not able to fully characterize such an effect near the Great Lakes due to the model's coarse spatial resolution. The aerosol vertical profiles measured by the newly launched Cloud-Aerosol Lidar and IR Pathfinder Satellite Observation (CALIPSO) satellite might provide valuable insight into how boundary layer mixing at local scales (~100-m spatial resolution, 20-km swath width) affects the association between total column AOD and ground-level $PM_{2.5}$ concentrations.

Estimated Formations of EPA $PM_{2.5}$ Constituents

Figure 3 shows the mean percentage contribution of each significant component to the concentrations of $PM_{2.5}$ and SO_4 in the east and west, and that of NO_3 in the west. Except for $PM_{2.5}$ concentrations in the east, which has a significant percentage of unexplained materials (31%) represented by the highly significant model intercept, the concentrations of other $PM_{2.5}$ constituents can be fully explained by different combination of MISR aerosol components. In the east, all the major MISR components present in the SO_4 model are also present in the $PM_{2.5}$

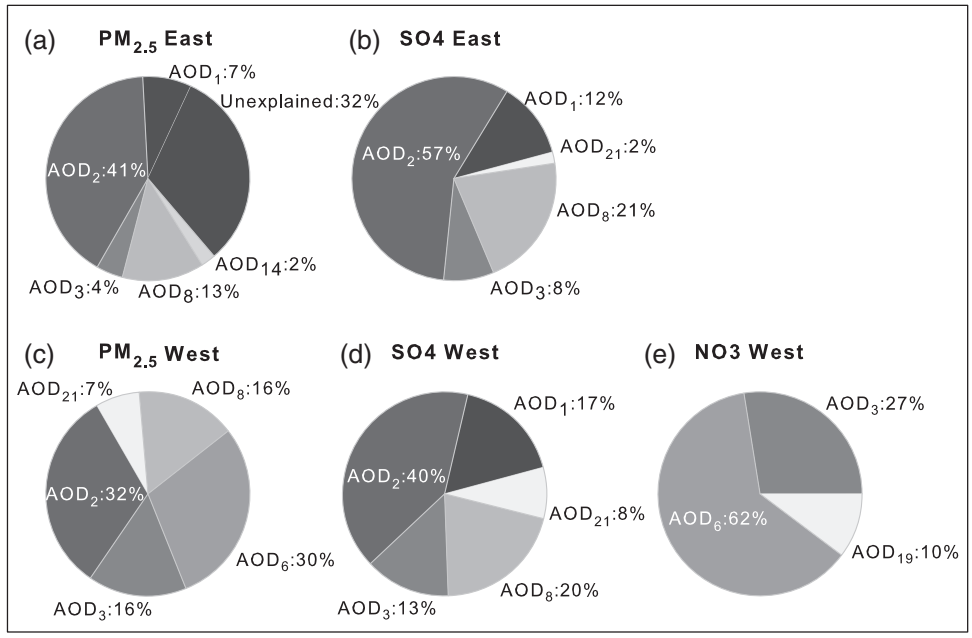

Figure 3. Contributions of significant MISR aerosol components (1, 2, etc.; see Table 1) to $PM_{2.5}$ mass in (a) the eastern and (c) western United States; SO_4 concentrations in (b) eastern and (d) western United States; and (e) NO_3 concentration in the western United States. The contributions only correspond to the proportion of these EPA measurements explained by the models.

model. Component 2 is the dominant contributor, providing nearly 41% of $PM_{2.5}$ mass and 57% SO_4 concentration. It is followed by components 8, 1, and 3 for both $PM_{2.5}$ and SO_4. This is probably due to the fact that sulfate particles represent a large fraction of total $PM_{2.5}$ mass in the east.

The significant MISR components in the SO_4 model are the same in east and the west except that the seasonal indicator is only significant in the east. This reflects the regional nature of sulfate particle pollution. The only difference is that in the west, larger particles such as components 3 and 21 have slightly greater contributions. The formation of $PM_{2.5}$ in the west is very different from that in the east, with components 2 and 6 both contributing approximately 30% to $PM_{2.5}$ mass, followed by larger particles such as components 3, 8, and 21. The large contribution of component 6 to $PM_{2.5}$ mass appears to come from NO_3, which has component 6 as its major contributor (54%). It is widely known that NO_3 concentrations in east are relatively low because of abundant sulfur dioxide (SO_2), which quickly consumes ammonia to form particle sulfate. Because of the lower SO_2 level, atmospheric conditions in the west are more favorable for the generation of ammonium nitrate (NH_4NO_3), thus NO_3 is a larger contributor to $PM_{2.5}$ mass in the west than in the east although regional features are also present. Our findings from the models agree with this consensus.

All the $PM_{2.5}$ constituents except NO_3 in the west include light-absorbing MISR aerosol components, such as components 8, 14, and 21. These components in the $PM_{2.5}$ may reflect that light-absorbing carbonaceous particles represent a substantial fraction of $PM_{2.5}$ mass. Their presence in the SO_4 formations is on one hand likely because of the immature status of retrieved aerosol microphysical properties in Version 17 MISR data. As shown in the companion paper, MISR is less sensitive in distinguishing light-absorbing particles from brighter particles. As a result, the presence of light-absorbing components in the SO_4 formations probably represents bright particles with similar size distributions and shapes that define the MISR light-absorbing components. As more mature MISR particle property products are becoming available, this issue is likely to be resolved. On the other hand, sulfate particles that are internally or externally mixed with carbonaceous particles could also cause the light-absorbing components to be significant in the model.

Estimated Particle Size Distributions

Figure 4 shows the size distribution for each of the four species calculated using the significant components in each regression model. Because smaller components account for over 90% of mass, the estimated $PM_{2.5}$ mass fraction in the east peaks at 0.19 μm. Also, the estimated size distribution supports the idea that particles smaller than 1 μm in size (i.e., the accumulation-mode particles) account for approximately 98% of the total $PM_{2.5}$ mass. Furthermore, the estimated size distributions of $PM_{2.5}$ and SO_4 are almost identical. In the west, the $PM_{2.5}$ mass fraction peaks at approximately 0.22 μm because of the presence of larger particles (i.e., component 6). There is a second mode beyond 2.5 μm, and the accumulation-mode particles account for approximately 62% of the

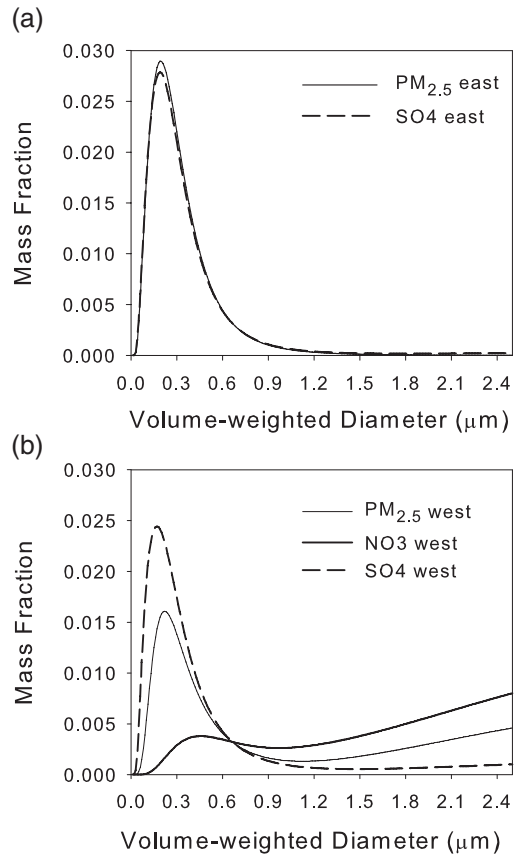

Figure 4. Estimated annual average size distribution of $PM_{2.5}$ and SO_4 in (a) the eastern United States, and (b) $PM_{2.5}$, SO_4, and NO_3 in the western United States.

$PM_{2.5}$ mass (see Figure 4). The estimated SO_4 size distributions have one peak around 0.17 μm, and accumulation mode particles account for 88% of the fine SO_4 mass. Because of the dominant presence of larger particles such as components 6 and 19, the NO_3 size distribution has one peak at 0.45 μm, and another peak beyond 2.5 μm. The accumulation-mode NO_3 particles only account for 25% of the fine NO_3 mass.

$PM_{2.5}$ size distributions are not routinely measured by the EPA compliance network, which limits us to only comparing the estimated size distributions with more general information in the literature. Previous studies of ground-level fine particle size distributions have reported that the accumulation mode often has a peak between 0.4 and 0.5 μm.[17,18] Our results for NO_3 generally agree with the reported peak size. They also capture reasonably well the difference between SO_4 and NO_3 size distributions, that is, accumulation-mode particles determine the SO_4 mass, whereas a significant proportion of NO_3 mass is in the coarse mode.[18] However, the estimated peak diameters of $PM_{2.5}$ mass and SO_4 particles are substantially smaller than those reported by ground measurements. One possible reason of this discrepancy is that MISR reports column-average aerosol microphysical properties. Because the mean RH level in the atmospheric column is substantially lower than in the boundary layer, the impact of particle growth on light scattering at ground level might not be fully captured in the regression models. This

discrepancy is more likely because satellite retrieved aerosol optical properties are naturally biased toward cloud-free days, because cloudy scenes are screened out to avoid situations when cloud-scattered light dominates the aerosol signal at the top of the atmosphere. The satellite sampling bias may cause the days when the droplet mode dominates the particle size distribution to be under-represented.

To evaluate the hypothesis of satellite sampling bias, we calculated the annual mean particle volume size distributions at two Aerosol Robotic Network (AERONET) sites (locations displayed in Figure 1) in 2005 using the Version 2 inversion data.[19,20] Particle density is unlikely to vary dramatically with particle size; therefore the volume size distribution is a good approximation to relative mass distribution. The AERONET inversion scheme assumes homogeneous aerosol vertical distribution. The results, reported in 22 size bins spread logarithmically between 0.05 and 15 μm, are then fit to one coarse and one fine mode, volume-weighted lognormal distributions. As shown in Figure 5, particle volume distribution peaks between 0.29 and 0.39 μm at the Goddard Space Flight Center (GSFC) site (eastern United States) and between 0.23 and 0.30 μm at the Rimrock site (western United States). These results are between our findings and those reported by ground measurements. Because AERONET radiometers take multiple measurements during the daytime, some measurements can still be made once the clouds move out of their fields of view. Therefore, particle growth linked to cloudy conditions is at least partially characterized in AERONET aerosol measurements. As a result, AERONET-estimated particle size distributions are less biased by the influences of cloud cover when compared with polar-orbiting satellites. This might be the reason that the AERONET-estimated peak particle sizes are slightly larger than those estimated by MISR. This provides evidence to our hypothesis that the smaller peaks of MISR estimated particle size is more likely because of satellite sampling bias than retrieval errors. Aircraft measurements of altitude-resolved particle size distributions, such as those over the Southern Great Plains,[21,22] could provide additional perspective on this issue. However, aircraft measurements must be combined with other data sources to support national or regional scale studies.

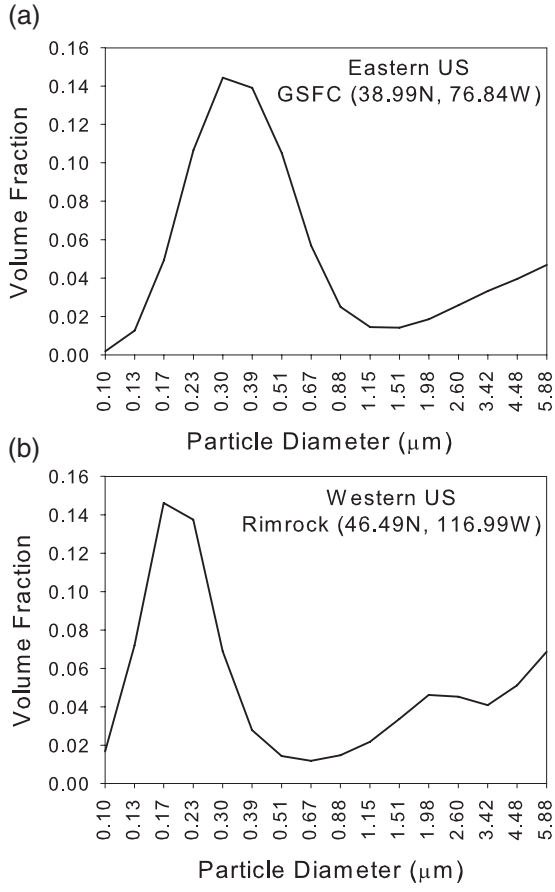

Figure 5. Annual average almucantar retrieval of particle volume size distributions in 2005 at two AERONET sites: (a) GSFC in the eastern United States and (b) Rimrock, ID in the western United States.

CONCLUSIONS

In this case study, we calculate the fractional AOD values for each MISR aerosol component using the mixtures selected in the MISR Version 17 aerosol product. We estimate the lower atmospheric proportions of the fractional AOD values by using GEOS-Chem simulated aerosol vertical profiles as scaling factors. These fractional AODs are used to predict ground-level concentrations of total $PM_{2.5}$ mass and major particle species measured at EPA's STN sites in 2005. This approach shows dramatic improvement in predicting power when compared with using the total column AOD as the sole predictor, ranging between 19 and 44% in the east, and more than 100% in the west. Regression analyses show that MISR aerosol components contribute differently to estimated $PM_{2.5}$ concentrations, and the significant components are different in the eastern and western United States. We are able to predict $PM_{2.5}$ mass and SO_4 concentrations in both the east and the west, and NO_3 concentrations in the west reasonably well, compared with available EPA ground-truth. The estimated $PM_{2.5}$ size distributions using the regression results capture the AERONET-derived overall pattern in both the east and west. However, due most likely to the sampling bias caused by cloud cover, estimated peak particle diameters tend to be smaller than those reported by ground measurements. Having demonstrated the power of this technique with an early version of the MISR particle microphysical property retrievals, future work will use more mature MISR particle property products now becoming available, and larger data samples that will allow greater stratification by season and location.

ACKNOWLEDGMENTS

This study is supported by the Harvard-EPA Center on Particle Health Effects (R-827353 and R-832416). The work of R. Kahn is supported in part by NASA's Climate and Radiation Research and Analysis Program, under H. Maring, and in part by the EOS-MISR instrument project; it is performed at the Jet Propulsion Laboratory at the California Institute of Technology under contract with NASA. We thank Dr. Lyatt Jeagle of the University of

Washington and Rynda Hudman of Harvard University for providing access to the GEOS-Chem NRT simulation results. We thank the continental U.S. AERONET site managers for providing their valuable data via the AERONET Web site (*http://aeronet.gsfc.nasa.gov*).

REFERENCES

1. Pope, C.A.; Dockery, D.W. Health Effects of Fine Particulate Air Pollution: Lines that Connect; *J. Air & Waste Manage. Assoc.* **2006**, *56,* 709-742.
2. Al-Saadi, J.; Szykman, J.; Pierce, R.B.; Kittaka, C.; Neil, D.; Chu, D.A.; Remer, L.; Gumley, L.; Prins, E.; Weinstock, L.; MacDonald, C.; Wayland, R.; Dimmick, F.; Fishman, J. Improving National Air Quality Forecasts with Satellite Aerosol Observations; *Bull. Am. Meteorol. Soc.* **2005**, *86,* 1249-1261.
3. Gupta, P.; Christopher, S.A.; Wang, J.; Gehrig, R.; Lee, Y.; Kumar, N. Satellite Remote Sensing of Particulate Matter and Air Quality Assessment Over Global Cities; *Atmos. Environ.* **2006**, *40,* 5880-5892.
4. Liu, Y.; Franklin, M.; Kahn, R.; Koutrakis, P. Using Aerosol Optical Thickness to Predict Ground-Level $PM_{2.5}$ Concentrations in the St. Louis Area: a Comparison between MISR and MODIS; *Remote Sens. Environ.* **2007**, *107,* 33-44.
5. Martonchik, J.V.; Diner, D.J.; Kahn, R.A.; Ackerman, T.P.; Verstraete, M.M.; Pinty, B.; Gordon, H. Techniques for the Retrieval of Aerosol Properties over Land and Ocean Using Multiangle Imaging; *IEEE Trans. Geosci. Remote Sens.* **1998**, *36,* 1212-1227.
6. Liu, Y.; Koutrakis, P.; Kahn, R. Estimating Fine Particulate Matter Component Concentrations and Size Distributions Using Satellite Retrieved Fractional Aerosol Optical Depth: Part 1—Method Development. *J. Air & Waste Manage. Assoc.* **2007**, *57*, 1351-1359.
7. Laden, F. Association of Fine Particulate Matter from Different Sources with Daily Mortality in Six U.S. Cities; *Environ. Health Perspect.* **2000**, *108,* 941-947.
8. Bey, I.; Jacob, D.J.; Yantosca, R.M.; Logan, J.A.; Field, B.D.; Fiore, A.M.; Li, Q.B.; Liu, H.G.Y.; Mickley, L.J.; Schultz, M.G. Global Modeling of Tropospheric Chemistry with Assimilated Meteorology: Model Description and Evaluation; *J. Geophys. Res. Atmos.* **2001**, *106,* 23073-23095.
9. Park, R. J.; Jacob, D. J.; Field, B. D.; Yantosca, R. M.; Chin, M. Natural and Transboundary Pollution Influences on Sulfate-Nitrate-Ammonium Aerosols in the United States: Implications for Policy. *J. Geophys. Res. Atmos.* **2004,** *109,* D15204.
10. Liu, Y.; Park, R.; Jacob, D.J.; Li, Q.; Kilaru, V.; Sarnat, J.A. Mapping Annual Mean Ground-Level $PM_{2.5}$ Concentrations using Multiangle Imaging Spectroradiometer Aerosol Optical Thickness over the Contiguous United States. *J. Geophys. Res. Atmos.* **2004**, *109*, D22206.
11. Liu, Y.; Sarnat, J.A.; Kilaru, V.; Jacob, D.J.; Koutrakis, P. Estimating Ground-Level $PM_{2.5}$ in the Eastern United States Using Satellite Remote Sensing; *Environ. Sci. Technol.* **2005**, *39,* 3269-3278.
12. Engel-Cox, J.A.; Holloman, C.H.; Coutant, B.W.; Hoff, R.M. Qualitative and Quantitative Evaluation of MODIS Satellite Sensor Data for Regional and Urban Scale Air Quality; *Atmos. Environ.* **2004**, *38,* 2495-2509.
13. Bond, T.C.; Bergstrom, R.W. Light Absorption by Carbonaceous Particles: an Investigative Review; *Aerosol Sci. Technol.* **2006**, *40,* 27-67.
14. Campanelli, M.; Delle, M.L.; Malvestuto, V.; Oliveiri, B. On the Correlation between the Depth of the Boundary Layer and the Columnar Aerosol Size Distribution; *Atmos. Environ.* **2003**, *37,* 4483-4492.
15. Andrews, E.; Saxena, P.; Musarra, S.; Hildemann, L.M.; Koutrakis, P.; McMurry, P.H.; Olmez, I.; White, W.H. Concentration and Composition of Atmospheric Aerosols from the 1995 SEAVS Experiment and a Review of the Closure between Chemical and Gravimetric Measurements; *J. Air & Waste Manage. Assoc.* **2000**, *50,* 648-664.
16. Frank, N.H. Retained Nitrate, Hydrated Sulfates, and Carbonaceous Mass in Federal Reference Method Fine Particulate Matter for Six Eastern U.S. Cities; *J. Air & Waste Manage. Assoc.* **2006**, *56,* 500-511.
17. Koutrakis, P.; Kelly, B.P. Equilibrium Size of Atmospheric Aerosol Sulfates as a Function of Particle Acidity and Ambient Relative-Humidity; *J. Geophys. Res. Atmos.* **1993**, *98,* 7141-7147.
18. Lestari, P.; Oskouie, A.K.; Noll, K.E. Size Distribution and Dry Deposition of Particulate Mass, Sulfate and Nitrate in an Urban Area; *Atmos. Environ.* **2003**, *37,* 2507-2516.
19. Dubovik, O.; King, M. D. A Flexible Inversion Algorithm for Retrieval of Aerosol Optical Properties from Sun and Sky Radiance Measurements; *J. Geophys. Res. Atmos.* **2000**, *105,* 20673-20696.
20. Dubovik, O.; Sinyuk, A.; Lapyonok, T.; Holben, B. N.; Mishchenko, M.; Yang, P.; Eck, T. F.; Volten, H.; Munoz, O.; Veihelmann, B.; van der Zande, W. J.; Leon, J. F.; Sorokin, M.; Slutsker, I. Application of Spheroid Models to Account for Aerosol Particle Nonsphericity in Remote Sensing of Desert Dust. *J. Geophys. Res. Atmos.* **2006**, *111,* D11208.
21. Andrews, E.; Sheridan, P. J.; Ogren, J.A.; Ferrare, R. In Situ Aerosol Profiles over the Southern Great Plains Cloud and Radiation Test Bed Site: 1. Aerosol Optical Properties. *J. Geophys. Res. Atmos.* **2004**, *109*, D06208.
22. Wang, J.; Collins, D.; Covert, D.; Elleman, R.; Ferrare, R.A.; Gasparini, R.; Jonsson, H.; Ogren, J.; Sheridan, P.; Tsay, S.C. Temporal Variation of Aerosol Properties at a Rural Continental Site and Study of Aerosol Evolution through Growth Law Analysis. *J. Geophys. Res. Atmos.* **2006**, *111,* D18203.

About the Authors

Yang Liu is a postdoctoral research fellow and Petros Koutrakis is a professor at the Harvard School of Public Health in Boston, MA. Ralph Kahn is a lead scientist for the Earth and Planetary Atmosphere Research Element at the Jet Propulsion Laboratory in Pasadena, CA. Solene Turquety is a CNES postdoctoral research fellow at the Université Pierre et Marie Curie in Paris, France. Robert M. Yantosca is a software engineer at Harvard Division of Engineering and Applied Sciences in Cambridge, MA. Please address correspondence to: Yang Liu, Harvard School of Public Health, Boston, MA 02215; phone: +1-617-384-8846; fax: +1-617-384-8859; email: yangliu@hsph.harvard.edu.